Modeling and Characterization of Cladding-Pumped Erbium-Ytterbium Co-doped Fibers for Amplification in Communication Systems

C. Matte-Breton, R. Ryf, N. K. Fontaine, R.-J. Essiambre, H. Chen, C. Kelly, Y. Messaddeq, and S. LaRochelle

IEEE/OSA Journal of Lightwave Technology, (Early Access) (2019)

Doi: 10.1109/JLT.2019.2961061

https://ieeexplore.ieee.org/abstract/document/8937826

Modeling and Characterization of Cladding-Pumped Erbium-Ytterbium Co-doped Fibers for Amplification in Communication Systems

C. Matte-Breton,[1] R. Ryf,[2] N. K. Fontaine,[2] R.-J. Essiambre,[2] H. Chen,[2] C. Kelly, Y. Messaddeq,[1] and S. LaRochelle[1]*

***Abstract*— Cladding-pumped optical fiber amplifiers are of increased interest in the context of space-division multiplexing but are known to suffer from low power efficiency. In this context, ytterbium (Yb) co-doping can be an attractive solution to improve the performance of erbium (Er) doped fiber amplifiers. We present a detailed direct comparison between Er/Yb-co-doping and Er-doping using numerical simulations validated by experimental results. Two double-cladding fibers, one doped with Er only and the other one co-doped with Er and Yb, were designed, fabricated and characterized. Using the experimentally extracted parameters, we simulate multi-core fiber amplifiers and investigate the interest of Er/Yb-co-doping. We calculate the minimum gain of the amplifiers over a 35-nm spectral window considering various scenarios.**

Index Terms*—Doped fiber amplifiers, Optical fiber networks, Space division multiplexing

I. Introduction

Space-division multiplexing (SDM) in optical communication systems is currently considered to overcome the capacity limit of optical fiber links [1,2]. Deploying SDM will require novel sub-systems, such as optical amplifiers, that will meet stringent performance requirements over all spatial channels. At this time, cladding-pumped optical fiber amplifiers offer the best solution in terms of simplicity and ease of integration in SDM links. Furthermore, cladding-pumping can be advantageously used to lower mode-dependent gain when using mode-division multiplexing over few mode fibers. In multi-core transmissions, cladding pumping avoids spatial channel demultiplexing/multiplexing at the amplifier input and allows the use of low-cost high-power multi-mode pump lasers. Although many research groups have recently demonstrated cladding-pumped multi-core amplifiers [3-9], one drawback of this technology remains its low pumping efficiency. How pumping efficiency translates into power efficiency depends on the specific amplifier designs, for example the number of cores in the cladding pumped amplifier. Similarly, a detailed comparison of the power consumption of multiple single core amplifiers to a multi-core cladding pumped amplifier will depend on the specific pumping scheme of the single core amplifiers, for example pump sharing among the amplifiers could reduce power cooling requirements. Comparison of power efficiency of the single-core versus multi-core approach is discussed in [10,11]. In this paper, we focus on the improvement of the pumping efficiency of multi-core cladding pumped amplifiers.

The low pumping efficiency of the cladding pumping geometry results from a significant decrease in the overlap between pump power and the erbium doped cores. Such decrease in the overlap results in the need to either (i) use very long fiber lengths, leading to important cost efficiency reduction, (ii) increase erbium doping concentration, leading to more clustering, or (iii) increase core density, leading to more crosstalk between the cores. Another possible solution is to use Er/Yb co-doping instead of only Er-doping in order to increase the absorption and pumping rates [12,13]. However, an important drawback with Er/Yb co-doping is that the presence of phosphorus in the doped region is required to suppress the back-transfer of energy from erbium to ytterbium by decreasing the non-radiative decay time from the $^4I_{11/2}$ to the $^4I_{13/2}$ energy level [14-19] and the presence of phosphorus and ytterbium in the glass matrix narrows the erbium absorption and emission cross-sections in the C-band (Fig. 6) [20-23]. An attempt to broaden the cross-sections by varying the aluminum concentration led to negligible change on the cross-sections [21]. Another way to broaden the cross-sections is to use fluoride phosphate glasses [24]. The issue with this method is that fluoride glass is very fragile and hard to handle, making it challenging to use commercially. Because of the narrow cross-sections, different portions of the C-band and L-band are commonly used instead of the typical 1530-1565 nm C-band in order to obtain a flat gain and achieve efficient power consumption in EYDFAs [25-26]. Indeed, despite the narrow cross-sections, wide band amplification can be achieved in

Manuscript received August 12, 2019; revised November 20, 2019. This work was supported in part by the Natural Sciences and Engineering Research Council of Canada (NSERC) and Alacatel Lucent Canada under Grant RDCPJ 515551-17.

C. Matte-Breton, Y. Messaddeq, and S. LaRochelle are with the Center for Optics, Photonics and Lasers (COPL), Department of Electrical and Computer Engineering, Université Laval, Québec, QC G1K 7P4, Canada (e-mail: sophie.larochelle@gel.ulaval.ca). R. Ryf, N. K. Fontaine, R.-J. Essiambre, and H. Chen are with Nokia Bell Labs, 791 Holmdel-Keyport Rd, Holmdel, NJ, 07733, USA. C. Kelly is with Nokia Canada, 600 March Rd, Ottawa, ON, K2K 2T6, Canada. Digital Object Identifier XX

National Science and Engineering Research Council of Canada (NSERC) Funding: RDCPJ 515551-17

EYDFAs by operating an amplifier in highly saturated conditions, leading to high gain toward the longer wavelengths, while the gain remains insufficient below 1535 nm. Using this principle, multiple MC-CP-EYDFAs have been demonstrated for wideband amplification [6-9,27].

In order to make Er/Yb-co-doped fiber amplifiers compatible with current communication networks, it is required to operate them with a flat gain over the entire C-band. By using a gain flattening filter (GFF) with up to 20 dB of depth, the amplifier gain can be flattened but at the expense of power efficiency. The gain after the GFF is limited by the channel with the minimum gain at the output of the doped fiber. The main issue with narrow cross-sections is therefore that the amplification of the channels with the highest gain will consume much of the pump power to generate high gain that will be thrown out by the GFF.

Since the minimum gain over the C-band is increased by a high pump absorption rate but decreased by the inefficient cross-sections shape, no "rule of thumb" exists to determine if and when Er/Yb-co-doping is advantageous compared to Er-doping. For a given pump power, this comparison might be done by determining the required fiber length for a given minimum gain or the minimum gain at the optimal fiber length.

In order to achieve a fair comparison between the two types of doping, ie. Er-doping vs Er/Yb-co-doping, numerical simulations must be executed with different scenarios. In this work, we consider a simple one-stage co-propagating pump amplifier. The residual pump power at the amplifier output is assumed to be discarded. The doped fiber parameters will be the same for the two Er/Yb-co-doped and Er-doped fiber designs except for the Yb ion concentration and the absorption/emission cross-sections that should differ according to the doping type. Our objective is to identify how to select the optimal doping for a C-band amplifier that maximizes the minimum gain at the optimal fiber length under given operating conditions such as input power, pump power and number of cores conditions. To our knowledge, this is the first detailed direct comparison between Er/Yb-co-doping and Er-doping, using simulations validated with experimental results, that investigates the interest of Er/Yb-co-doping in CP-MC-FAs (cladding-pumped multicore fiber amplifiers) in terms of minimum gain over the 1530-1565 nm C-band. In section II, we introduce the model of the Er-doped and Er/Yb-co-doped amplifiers. In section III, a single-core erbium-ytterbium doped fiber (EYDF) and a single-core erbium doped fiber (EDF) are fabricated and characterized. Then, the gain and noise figure (NF) of the fibers are compared with simulation results to validate the model in section IV. Finally, with the experimentally extracted parameters, section V calculates the performances of cladding-pumped multicore erbium doped fiber amplifiers (CP-MC-EDFAs) and cladding-pumped multicore erbium-ytterbium doped fiber amplifiers (CP-MC-EYDFAs) in order to conclude on the interest of CP-MC-EYDFAs for communication systems.

II. Modeling of Doped Fiber Amplifiers

The model is based on the standard set of power propagation and population rate equations of Er/Yb-co-doped fibers, as described in [15,28-30], that neglects back-transfer and considers only the Er^{3+} $I_{15/2}$ and $I_{13/2}$ energy levels. This was proven to be a valid assumption in phosphate glass hosts and in silica-based fibers with small amounts of phosphorus in the doped region [14-19]. Rather than using population average over the transverse cross-section, we introduce radial resolution of the rare-earth ion populations as described in [20,31]. Since our aim is to design single-mode amplifiers, only the LP_{01} mode is considered in the simulations for the signal. The pump power is assumed to be uniformly distributed in the cladding that is D-shaped and has a diameter across the core of 125 μm (105 μm perpendicular to the flat portion). Consequently, there is no azimuthal dependence and we divide the fiber cross-section in K rings, each with uniform Er^{3+} concentration, and we calculate the inversion of each ring to calculate transition rates and gain. We also neglect background propagation loss. The propagation of the pump power, P_p, the signal, P_s, and the ASE, $P^{\pm}_{ASE}$, in the forward (+) and backward (-) direction are described by

$$\begin{cases} \dfrac{dP_p(z)}{dz} = -\left(\sigma_{ap,Er}\left(\sum_{k=1}^{K} n_{1,Er,k}(z)\,\Gamma_{p,k}\right) + \sigma_{ap,Yb}\left(\sum_{k=1}^{K} n_{1,Yb,k}(z)\,\Gamma_{p,k}\right)\right)P_p(z \\ \dfrac{dP_{s,\lambda}(z)}{dz} = \left(\sigma_{e,Er,\lambda}\sum_{k=1}^{K} n_{2,Er,k}(z)\,\Gamma_{\lambda,k} - \sigma_{a,Er,\lambda}\sum_{k=1}^{K} n_{1,Er,k}(z)\,\Gamma_{\lambda,k}\right)P_{s,\lambda}(z) \\ \dfrac{dP^{\pm}_{ASE,\lambda}(z)}{dz} = \left(\sigma_{e,Er,\lambda}\sum_{k=1}^{K} n_{2,Er,k}(z)\,\Gamma_{\lambda,k} - \sigma_{a,Er,\lambda}\sum_{k=1}^{K} n_{1,Er,k}(z)\,\Gamma_{\lambda,k}\right)P^{\pm}_{ASE,\lambda}(\\ \qquad +\sigma_{e,Er,\lambda}\left(\sum_{k=1}^{K} n_{2,Er,k}(z)\,\Gamma_{\lambda,k}\right)2h\nu_\lambda\Delta\nu_\lambda \end{cases} \quad (1)$$

where λ stands for the wavelength channel of the signal or the amplified spontaneous emission (ASE), and k refers to the different rings with area A_k. Also, $\sigma_{ap,Er}$ and $\sigma_{ap,Yb}$ are the absorption cross-sections at 976 nm for Er^{3+} and Yb^{3+} respectively, $\sigma_{e,Er,\lambda}$ and $\sigma_{a,Er,\lambda}$ are the emission and absorption cross-sections at the signal or ASE wavelengths for Er^{3+}. The pump and signal (or ASE) overlaps with each ring are $\Gamma_{p,k}$, and $\Gamma_{\lambda,k}$ respectively. As usual, h is Planck constant, ν_p and ν_λ are the pump and signal (or ASE) frequency. The radially resolved population inversion along the fiber are given by

$$\begin{cases} n_{2,Er,k}(z) = \dfrac{\left(W_{1,k}(z) + W_{2,k}(z) + A_k K_{tr} n_{2,Yb,k}(z)\right)\rho_{Er,k}(z)}{W_{1,k}(z) + W_{2,k}(z) + W_{3,k}(z) + A_k K_{tr} n_{2,Yb,k}(z) + \dfrac{A_k}{\tau_{Er}}} \\ n_{2,Yb,k}(z) = \dfrac{\left(W_{4,k}(z)\right)\rho_{Yb,k}(z)}{W_{4,k}(z) + A_k K_{tr} n_{2,Yb,k}(z) + \dfrac{A_k}{\tau_{Yb}}} \\ \rho_{Er,k}(z) = n_{1,Er,k}(z) + n_{2,Er,k}(z) \\ \rho_{Yb,k}(z) = n_{1,Yb,k}(z) + n_{2,Yb,k}(z) \end{cases} \quad (2)$$

where the lower and upper level population densities of a given ring are $n_{1,Er,k}$ and $n_{2,Er,k}$ for Er^{3+} and $n_{1,Yb,k}$ and $n_{2,Yb,k}$ for Yb^{3+}, while $\rho_{Er,k}$ and $\rho_{Yb,k}$ are the Er^{3+} and Yb^{3+} concentrations of a given doped ring. The lifetime of the Er^{3+} and Yb^{3+} upper metastable levels are τ_{Er} and τ_{Yb}. It can be found in the literature that the lifetime of these upper metastable levels are generally around 10 ms and 1.5 ms for erbium and ytterbium [20]. These

National Science and Engineering Research Council of Canada (NSERC) Funding: RDCPJ 515551-17

lifetimes will not be characterized and we will rather use values found in the literature for our simulations. Also, K_{tr} is the energy-transfer rate from ytterbium to erbium. Finally, the transition rates associated with pump absorption by erbium (W_1), signal and ASE absorption by erbium (W_2), signal and ASE stimulated emission by erbium (W_3) and pump absorption by ytterbium (W_4) are written as

$$\begin{cases} W_{1,k}(z) = \dfrac{\sigma_{ap,Er}\Gamma_{p,k}P_p(z)}{h\nu_p} \\ W_{2,k}(z) = \displaystyle\sum_{\lambda,s}\frac{\sigma_{a,Er,\lambda}\Gamma_{\lambda,k}P_{s,\lambda}(z)}{h\nu_\lambda} + \sum_{\lambda,ASE}\frac{\sigma_{a,Er,\lambda}\Gamma_{\lambda,k}P_{ASE,\lambda}(z)}{h\nu_\lambda} \\ W_{3,k}(z) = \displaystyle\sum_{\lambda,s}\frac{\sigma_{e,Er,\lambda}\Gamma_{\lambda,k}P_{s,\lambda}(z)}{h\nu_\lambda} + \sum_{\lambda,ASE}\frac{\sigma_{e,Er,\lambda}\Gamma_{\lambda,k}P_{ASE,\lambda}(z)}{h\nu_\lambda} \\ W_{4,k}(z) = \dfrac{\sigma_{ap,Yb}\Gamma_{p,k}P_p(z)}{h\nu_p} \end{cases} \quad (3)$$

For the simulations of the Er-doped fiber, $\rho_{Yb,k}$, K_{tr} and $\sigma_{ap,Yb}$ is set to 0, whereas for the simulation of the Er/Yb-co-doped fiber the absorption of the Er^{3+} is considered negligible compared to the absorption of Ytterbium and $\sigma_{ap,Er}$ is thus set to 0.

III. Fabrication and Parameter Characterization of an EYDF and an EDF

An EYDF (fiber A) and an EDF (fiber B) were fabricated using the solution doping method [32] with Al_2O_3, P_2O_5, Er_2O_3 and Yb_2O_3 in the case of fiber A; and Al_2O_3 with Er_2O_3 in the case of fiber B (Fig.1). The fibers were designed to have the same refractive index profile and the same erbium concentration profile. In the EYDF, the target Yb^{3+} concentration in ions/m^3 was 10 times higher than the Er^{3+} concentration, and the phosphorus concentration was 100 times higher than the Er^{3+} concentration. The Al_2O_3 concentration was used to control the refractive index profile. The preforms were polished in order to obtain D shaped fibers to break the symmetry of the pump modes guided by the cladding and the silica cladding was surrounded by a low refractive index polymer (n=1.37). For both fibers, the silica cladding diameter was 125 µm (105 µm when measured perpendicular to the flat section).

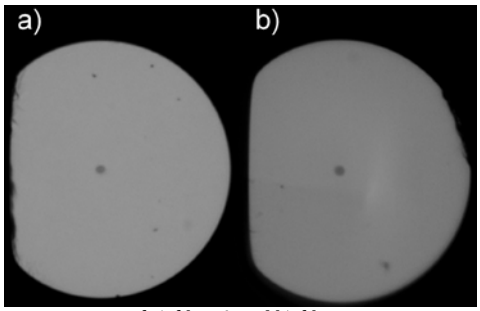

Fig. 1. Microscope image of a) fiber A and b) fiber B.

The core refractive index profile was measured on the preforms with a NR-9200HR refracted near-field analyzer (EXFO) at 657.6 nm. To apply the measurement results to the C-band, we neglect the dispersion of the refractive index difference between the core and the glass cladding, Δn. Also, we scale the radial position using the diameter ratio of the fabricated fiber and the preform. The resulting refractive index profiles of fiber A and B are shown in Fig. 2. The dip at the center of the core in fiber A is caused by evaporation during the MCVD process. The higher evaporation could be caused by the presence of Yb_2O_3 and P_2O_5 in the glass matrix.

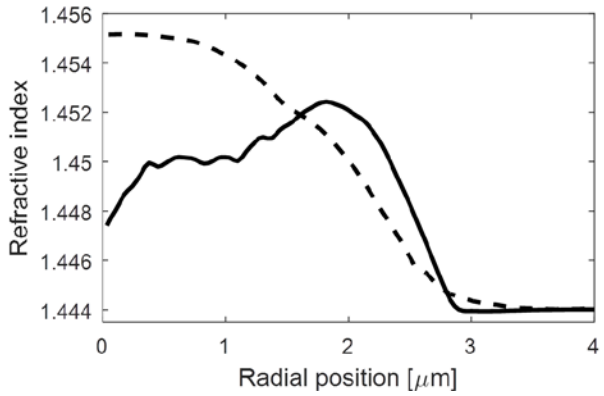

Fig. 2. Refractive index profile of fiber A (solid) and fiber B (dashed).

With the measured refractive index profiles, we used COMSOL to calculate the LP_{01} mode overlap with 30 rings of 0.1 µm thickness located in the 0-3 µm radial position of the fiber. The calculations were executed for wavelengths between 1420 nm to 1620 nm for fiber A and fiber B and are shown in Fig. 3. The pump overlap in each ring was calculated by considering a uniform pump power distribution over the fiber. Considering that both fibers have the same D-shape with a cladding area of 1.003×10^{-8} m^2, the pump overlap with each ring is the same for both fibers and is directly proportional to the area of the ring, i.e., to a first approximation, proportional to the radius of the ring.

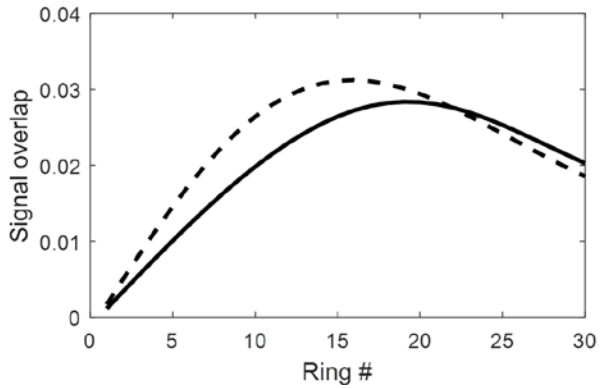

Fig. 3. Signal overlap with each ring in fiber A (solid) and fiber B (dashed) at 1550 nm.

The doping concentrations of Er^{3+}, Yb^{3+} and P_2O_5 were measured on the preform at different radial positions using an electron micro probe analyzer. As before, the radial position was scaled using the diameter ratio of the fabricated fiber and the preform and the erbium and ytterbium measured concentrations are shown in Fig. 4. While not used in the simulations, note that the phosphorus concentration was, on average, 1.2×10^{27} m^{-3} in the core region of fiber A.

National Science and Engineering Research Council of Canada (NSERC) Funding: RDCPJ 515551-17

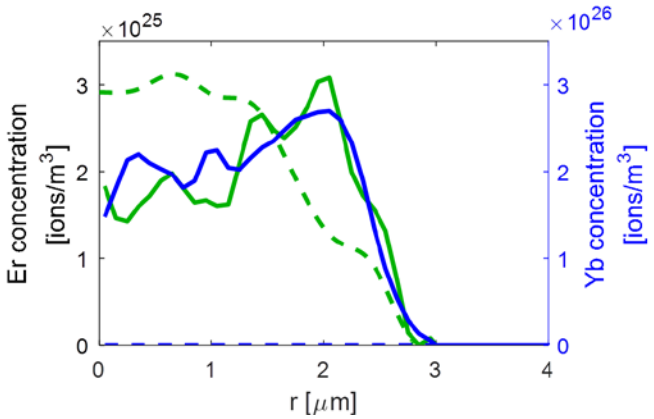

Fig. 4. Erbium (green) and ytterbium (blue) concentration profile of fiber A (solid) and fiber B (dashed).

Using a supercontinuum laser source with an average of approximately -35 dBm/nm output power over the 1420 nm – 1620 nm region, we injected the light in the core of the EYDF (fiber A) and EDF (fiber B) by splicing the output fiber of the supercontinuum at the input of the fiber under test (FUT) and measuring the output power of the FUT as a function of wavelength on an optical spectrum analyzer (OSA, 1 nm resolution). Then, the difference between the input and output power was calculated and divided by the fiber length used. Fiber lengths of 80 cm for fiber A and 70 cm for fiber B were used. The resulting absorption curves, as a function of wavelength, are shown in Fig. 5.

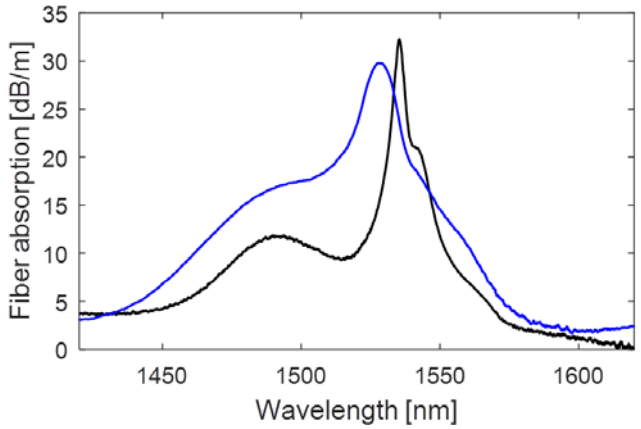

Fig. 5. Absorption as a function of wavelength from 1420 nm to 1620 nm for fiber A (black) and fiber B (blue).

Knowing the LP_{01} overlap and the Er^{3+} concentration profile of each ring in fibers A and B, the absorption and emission cross-sections were calculated with the McCumber relation, see [33] for example, written as

$$\sigma_a(\nu)[m^2] = \frac{\alpha\,[dB/m]}{(10\,log_{10}e)\sum_k \rho_k[ions/m^3]\Gamma_k} \quad (4)$$

$$\sigma_e(\nu) = \sigma_a(\nu)e^{(\varepsilon-h\nu)/k_BT} \quad (5)$$

$$\varepsilon = \frac{hc}{\lambda_\varepsilon} \quad (6)$$

In Eq. (4) to (6), σ_a is the absorption cross-section, α is the measured absorption, ρ_k is the doping concentration in the ring k, Γ_k is the power confinement in the ring k, σ_e is the emission cross section, ν is the optical frequency, c is the speed of light, ε is the mean transition energy between two manifolds, T is the equilibrium temperature and k_B is the Boltzmann constant. The mean wavelength at which the transition occurs, λ_ε, is generally close to the peak absorption value. We set λ_ε to 1535 nm for fiber A and 1532 nm for fiber B in order to obtain cross-sections in agreement with the literature [18, 22-23]. The resulting cross-sections are shown in Fig. 6.

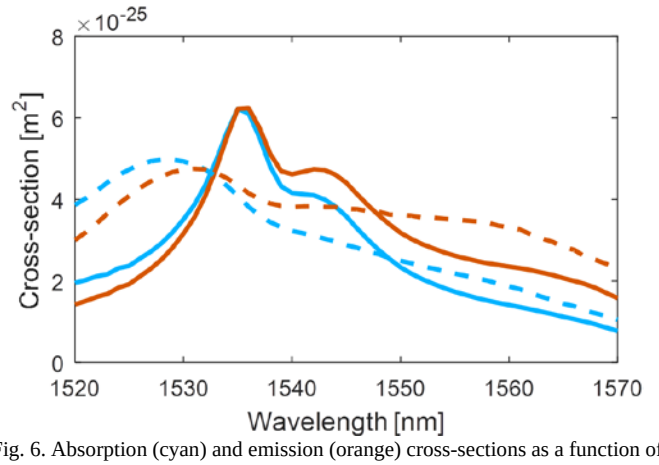

Fig. 6. Absorption (cyan) and emission (orange) cross-sections as a function of wavelength from 1520 nm to 1570 nm for fiber A (solid lines) and fiber B (dashed lines).

In order to measure the absorption cross-section near 976 nm, we injected the light of a supercontinuum laser source with an average of approximately -42 dBm/nm output power over the 880 nm – 1000 nm region in the cladding of fiber A and a supercontinuum laser source with an average of -36 dBm/nm output power over the 800 nm – 1300 nm region in the cladding of fiber B and measured the output power with an OSA (1 nm resolution). We used 15 m of fiber A and 183 m of fiber B. Absorption was estimated as the loss difference with respect to the measurement at 880 nm in order to substract background loss and the result is shown in Fig. 7. Since the pump source that will be used for the gain measurements is centered at 976 nm, we compute the absorption average from 974 nm to 978 nm of both fibers and obtained 0.785 dB/m for fiber A and 0.0394 dB/m for fiber B. Using the measured Yb^{3+} (for fiber A) and the Er^{3+} (for fiber B) concentration in each ring, we calculated the respective absorption cross-sections near 976 nm were calculated and found $\sigma_{ap,Yb} = 3.86\times10^{-25}$ m^2 for fiber A and $\sigma_{ap,Er} = 2.25\times10^{-25}$ m^2 for fiber B. For fiber B, the absorption peak at 943 nm is caused by the absorption from OH- impurities over the 183 m of fiber used. Although it cannot be distinguished properly because of the scale of the y axis, the same peak is observed on the absorption curve of fiber A. The transfer rate from Yb^{3+} to Er^{3+} upper metastable levels K_{tr} in fiber A could not be characterized and will be determined by fitting the gain measurements of the EYDF in the section IV.

National Science and Engineering Research Council of Canada (NSERC) Funding: RDCPJ 515551-17

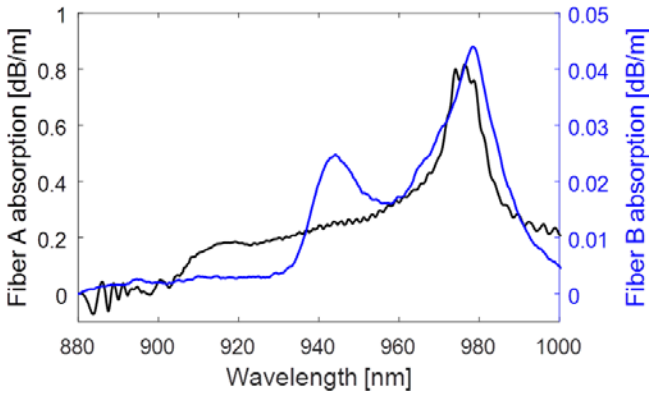

Fig. 7. Absorption in the cladding as a function of wavelength from 880 nm to 1000 nm for fiber A (black) and fiber B (blue).

The signal background loss was measured at 1700 nm by injecting the light of a supercontinuum laser source with an average of approximately -40 dBm/nm output power in the core of the fiber under test and measured the output power with an OSA (1 nm resolution). We used 100 m of fiber A and 172 m of fiber B and measured a signal background loss of 0.099 dB/m for fiber A and 0.039 dB/m for fiber B. The pump background loss was measured at 880 nm with a supercontinuum laser source with an average of -36 dBm/nm output power over the 800 nm – 1300 nm region and a fiber length of 113 m for fiber A and 183 m for fiber B.

IV. Gain and NF: Model Validation

In this section, we perform experimental characterization of the two single core cladding-pumped doped fibers: fiber A (EYDF) and fiber B (EDF). The experimental results served to validate the model and the fiber parameters that will be used to compare MC-CP-EYDFAs with MC-CP-EDFAs through numerical simulations in section V and section VI. We spliced 3.36 m of fiber A and 3.50 m of fiber B to standard single-mode fiber (SMF) pigtails at both ends. We measured a 2.1 dB total loss for the two splices and connectors using a tunable laser set at 1640 nm and -5 dBm. In the calculation of the internal gain and NF, we assume that 1.05 dB loss occurs before the doped fibers and 1.05 dB after. Right after the first splice, the DFUT (doped fiber under test) was stripped over 20 cm. Then, a coreless fiber, spliced on the output fiber of the pump laser diode, is tapered and rolled around the DFUT in order to achieve side-coupling of the pump power in the cladding of the DFUT. Starting about 1 cm from the output splice, a glass etching cream (Armour Etch #15-0150) is applied over four cm in order to make the surface of the fiber irregular which removes the pump through surface scattering. Overall, approximately 10 cm of the DFUT is not pumped significantly, a few centimeters before the pump coupling and a few centimeters after the pump dump. Thus, for the simulations, we consider 3.26 m of fiber length for fiber A and 3.40 m for fiber B.

Fig. 8. Setup used to measure the gain and NF of fiber A and B.

The setup used for the gain and NF measurements is shown in Fig. 8. The 14 channels are distributed uniformly from 1531.2 nm to 1562.2 nm with 300 GHz spacing. The total signal input power is set to -15 dBm (-26.46 dBm/ch), -5 dBm (-16.46 dBm/ch) and 5 dBm (-6.46 dBm/ch). The output power of the pump laser diode is set to 3 W, 5 W and 7 W. The pump power coupling efficiency is measured after the gain and NF measurements are completed by cutting the fiber 40 cm after the input splice to measure the 976 nm power when the pump is set to 5 W. We measured 2.35 W for fiber A and 2.40 W for fiber B, which leads to pump power coupling efficiencies of 47% and 48%. These coupling efficieny values are used for the simulations. Also, for the simulations, the C-band is loaded with 32 channels uniformly distributed between 1531 nm and 1562 nm with 1 nm spacing. As in the experiments, the total signal input power is set to -15 dBm, -5 dBm and 5 dBm. The transition rate from ytterbium to erbium (K_{tr}) was set to $1.0\text{x}10^{-22}$ m^3/s. This value was determined by minimizing the error between gain measurements and simulations with coupled pump power of 3.29 W and input signal power of 5 dBm for fiber A. This value compares well to the literature [20]. All of the fibers parameters are summarized in Table 1.

Fig. 9 and Fig. 10 compare simulations and measurements of gain and NF for fiber A and B respectively. For both the gain and NF measurements, the insertion loss of the components and splices are considered in order to determine the internal gain and the internal NF, which is what is directly obtained with the simulations. A good agreement is observed between measurements and simulations with a maximum gain difference of <2.4 dB for fiber A and <2.7 dB for fiber B, and a maximum NF difference of <2 dB for fibers A and B. When using cladding pumping, because of the small core sizes, the pump overlap with the cores is low and leads to poor gains for both fibers. In the next section, we will use these values to design MC-CP-EYDFA and the core sizes will be adjusted accordingly.

National Science and Engineering Research Council of Canada (NSERC) Funding: RDCPJ 515551-17

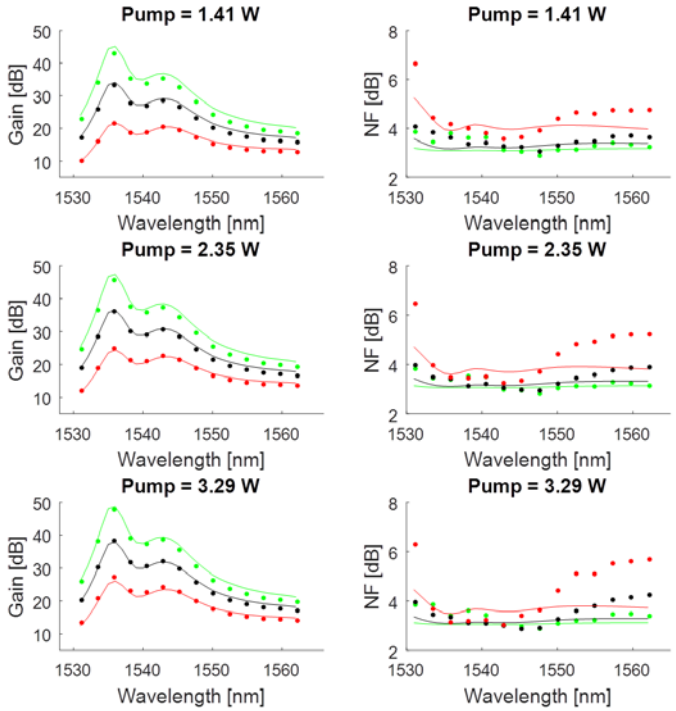

Fig. 9. Measured (markers) and simulated (solid lines) gain (left) and NF (right) of fiber A for input power of -15 dBm (green), -5 dBm (black) and 5 dBm (red) with coupled pump power of 1.41 W (top), 2.35 W (center) and 3.29 W (bottom).

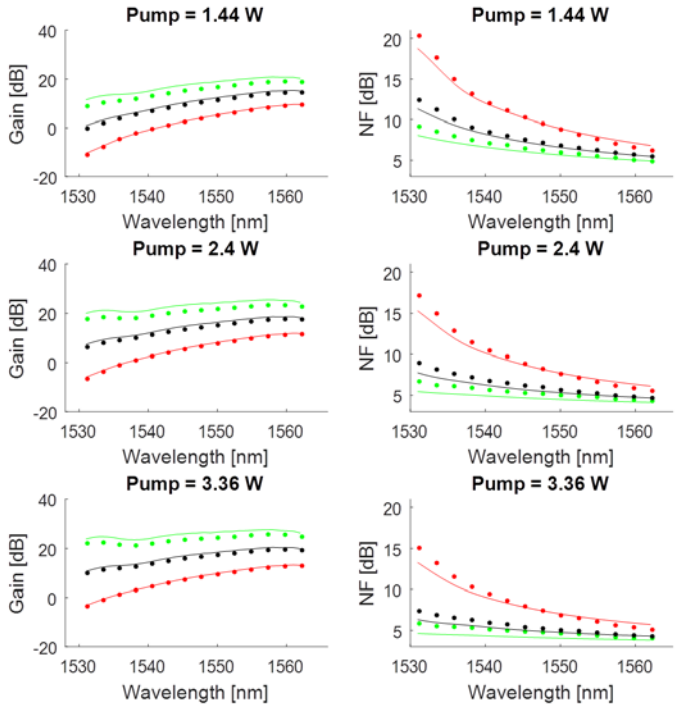

Fig. 10. Measured (markers) and simulated (solid lines) gain (left) and NF (right) of fiber B for input power of -15 dBm (green), -5 dBm (black) and 5 dBm (red) with coupled pump power of 1.44 W (top), 2.40 W (center) and 3.36 W (bottom).

TABLE I
FIBERS PROPERTIES

Parameter	Value		Unit
	Fiber A	Fiber B	
L	3.36	3.50	m
N_{cores}	1	1	-
$\Gamma_{\lambda,k}$	Fig. 3.	Fig. 3.	-
$\Gamma_{p,k}$	Ring area/cladding area		-
$\rho_{k,Er}$	Fig. 4.	Fig. 4.	ions/m^3
$\rho_{k,Yb}$	Fig. 4.	-	ions/m^3
$\sigma_{a,\lambda}$	Fig. 6.	Fig. 6.	m^2
$\sigma_{e,\lambda}$	Fig. 6.	Fig. 6.	m^2
$\sigma_{ap,Er}$	-	2.25×10^{-25}	m^2
$\sigma_{ap,Yb}$	3.86×10^{-25}	-	m^2
τ_{Er}	10	10	ms
τ_{Yb}	1.5	-	ms
K_{tr}	1.0×10^{-22}	-	m^3/s

V. INTEREST OF MC-CP-EYDFA FOR COMMUNICATIONS

In order to investigate the interest of MC-CP-EYDFAs for communications, we use the same model but with seven cores sharing the available pump instead of one. The signal in each core consists of 31 channels, from 1530 nm to 1560 nm. Some of the characterization results obtained in section IV are used for the simulation based comparison of MC-CP-EYDFAs with MC-CP-EDFAs. More specifically, the absorption and emission cross-sections, the lifetime of Er^{3+} and Yb^{3+} upper metastable levels, and the energy-transfer rate from ytterbium to erbium (K_{tr}) of the CP-MC-EYDFAs and the CP-MC-EDFAs are the same as fiber A and fiber B respectively. For these simulations, we assume ideal refractive index and doping profiles. The fiber cores are 6 µm diameter step-index cores with Δn = 0.013. The Er^{3+} concentration is uniform over the core region and set to $2x10^{25}$ ions/m^3. The Yb^{3+} concentration is set to $2x10^{26}$ ions/m^3 in the cores of the CP-MC-EYDFAs and to 0 ions/m^3 for CP-MC-EDFAs.

National Science and Engineering Research Council of Canada (NSERC) Funding: RDCPJ 515551-17

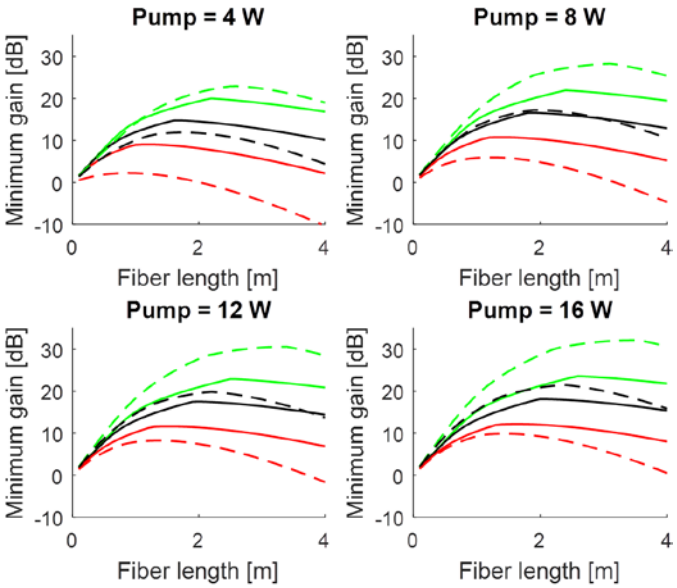

Fig. 11. Simulated gain of a CP-MC-EYDFA (solid) and a CP-MC-EDFA (dashed) for input signal power of -15 dBm (green), -5 dBm (black) and 5 dBm (red) with coupled pump power of a) 4 W, b) 8 W, c) 12 W and d) 16 W and 7 cores sharing the pump.

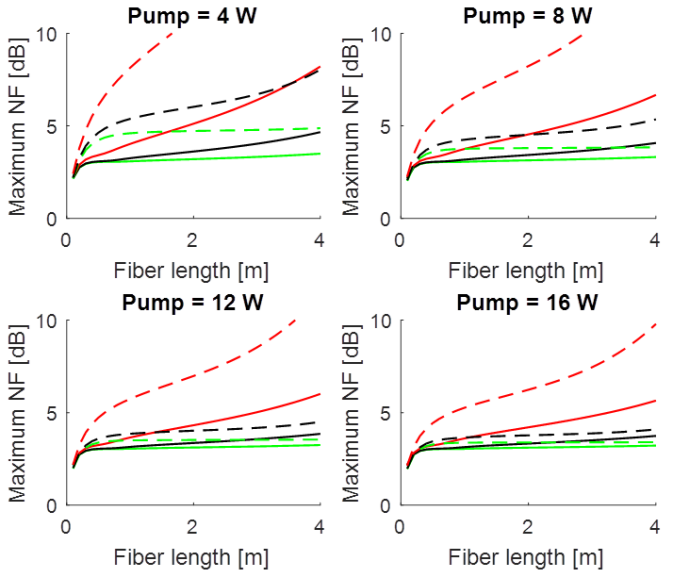

Fig. 12. Simulated NF of a CP-MC-EYDFA (solid) and a CP-MC-EDFA (dashed) for input signal power of -15 dBm (green), -5 dBm (black) and 5 dBm (red) with coupled pump power of a) 4 W, b) 8 W, c) 12 W and d) 16 W and 7 cores sharing the pump.

In order to investigate if Er/Yb-co-doping can lead to a higher minimum gain over 1530 nm to 1560 nm region, we plot the minimum gain as a function of fiber length for different operating conditions of CP-MC-EYDFAs and CP-MC-EDFAs. The results are shown in Fig. 11 for different pump input power and different signal input power. From these results, we see that CP-MC-EYDFA will lead to higher minimum gain, compared to CP-MC-EDFA, when there is a higher signal power or a lower pump power, which are the conditions that lead to saturation of CP-MC-EDFA. On Fig. 12, the maximum NF over the 1530 nm to 1560 nm region is shown for the same scenarios as Fig. 11. For all the scenarios where Er/Yb-codoping allows to reach a higher minimum gain compared to Er-doping, Er/Yb-codoping also allows to keep the NF lower. It thus seems that the use of CP-MC-EYDFAs could be of interest when the available pump power is limited, for example in subsea networks. Although the minimum gain can be very similar, gain variations across the C-band can be very different. For example, for the -5 dBm input signal power and 8 W input pump power scenario, the minimum gain over the 1530-1560 nm region is almost the same for both fibers (16.6 dB vs 17.3 dB for the CP-MC-EYDFA and the CP-MC-EDFA respectively) and occurs at approximately the same fiber length (1.8 m and 1.9 m for the for the CP-MC-EYDFA and the CP-MC-EDFA). Under these conditions, the average upper state population over the total length of the fiber is 71.6% for the CP-MC-EYDFA and 63.8% for the CP-MC-EDFA. The spectral gain variations in the CP-MC-EYDFA are therefore much larger, as shown in Fig. 13, and would require a GFF with >15 dB of depth. However, the maximum NF over this spectral window for fiber A is only 3.4 dB compared to 4.5 dB for fiber B.

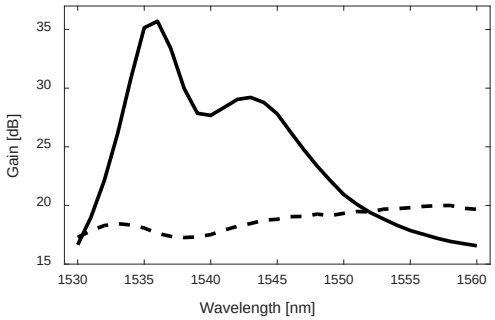

Fig. 13. Simulated gain of a seven-core CP-MC-EYDFA (solid) and a CP-MC-EDFA (dashed) for input signal power of -5 dBm, input pump power of 8 W.

VI. Optimal Wavelength Range for MC-CP-EYDFAs

In this section, we investigate what is optimum transmissions 30-nm window of CP-MC-EYDFA vs CP-MC-EDFA. We first perform simulations of CP-MC-EYDFA using the same fiber parameters as in section V. For each spectral region, two scenarios are considered: a) 8 W input pump power and -5 dBm input signal power, and b) 16 W input pump power and -5 dBm input signal power. For both scenarios, the minimum gain over the spectral region is plotted as a function of fiber length in Fig. 14. The results shown in this section are the internal gain and the internal NF. In order to determine the total amplifier gain and NF for a given application, the loss of isolators, splices and other sources of loss should also be considered.

The results indicate that the optimal 30-nm wide wavelength range for CP-MC-EYDFA is 1536 nm – 1566 nm. However, it is worth noticing that the 1535 nm – 1565 nm wavelength range gives a very similar result while being inside the C-band. When compared to the CP-MC-EDFA results shown on Fig. 11, the Er/Yb-co-doping results lead to better gain and pump efficiency. Due to the lower emission cross-section at the higher wavelengths, a longer fiber is also required. Note that for 8 W input pump power, the optimal length for the EYDFA is 6.1 m and the minimum gain is 26.2 dB.

National Science and Engineering Research Council of Canada (NSERC) Funding: RDCPJ 515551-17

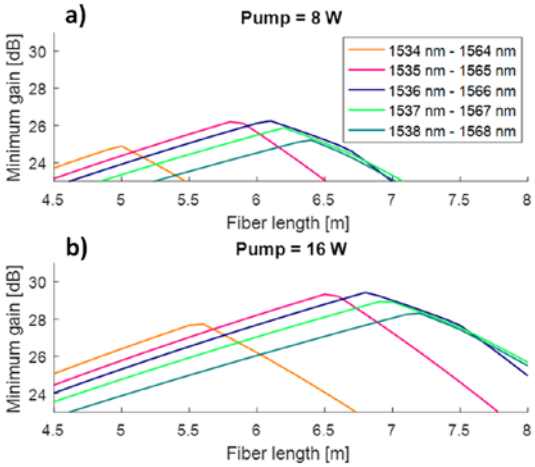

Fig. 14. Simulated minimum gain of a CP-MC-EYDFA for different 30-nm spectral windows with input signal power of -5 dBm and input pump power of a) 8 W, b) 16 W.

At the optimal fiber length, the maximum NF calculated over the wavelength range of the various scenarios shown on Fig. 14 was <3.5 dB for a pump power of 8 W and <3.4 dB for a pump power of 16 W (with variations less than 0.1 dB among the tested wavelength ranges). The only noticeable increase in NF occurred when the fiber length was much longer than the optimal length.

If we repeat the same experiment for MC-CP-EDFAs, we find an optimal wavelength range of 1531– 1561 nm, and an optimal minimum gain of 17.6 dB for 2.2 m of fiber length, 8 W of input pump power and -5 dBm of input signal power. The gain curve of the MC-CP-EYDFA and MC-CP-EDFA at their optimal fiber length over their optimal 30-nm wide spectral region is shown on Fig. 15.

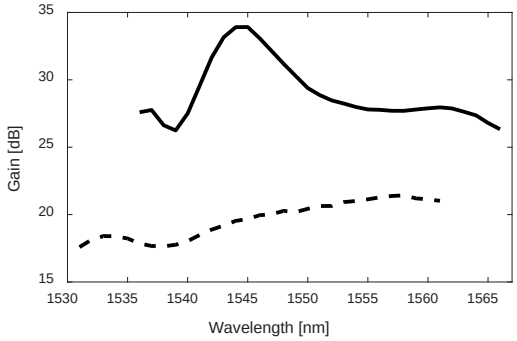

Fig. 15. Simulated gain of a CP-MC-EYDFA (solid) and a CP-MC-EDFA (dashed) for input signal power of -5 dBm, input pump power of 8 W, and 7 cores. The results were obtained with fiber lengths of 6.1 m for the CP-MC-EYDFA and 2.2 m for the CP-MC-EDFA over the respective 30-nm spectral windows from 1536 – 1566 nm and 1531 – 1561 nm.

Similarly, we found that when a 35-nm transmission window is desired, the optimal wavelength range is 1535 – 1570 nm for EYDFAs and 1532 – 1567 nm for EDFAs. The calculated gain spectra at 8 W with the optimal fiber lengths are shown in Fig. 16 and the resulting minimum gain is 23.1 dB for the EYDFA and 17.7 dB for the EDFA.

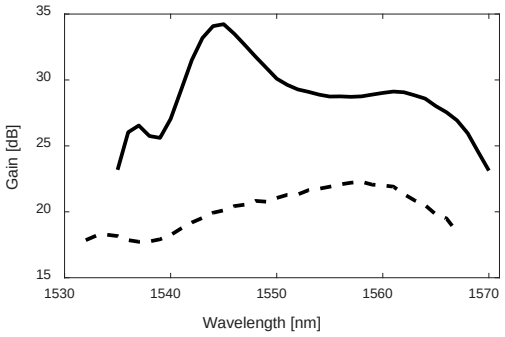

Fig. 16. Simulated gain of a CP-MC-EYDFA (solid) and a CP-MC-EDFA (dashed) for input signal power of -5 dBm, input pump power of 8 W, and 7 cores. The results were obtained with fiber lengths of 6.6 m for the CP-MC-EYDFA and 2.4 m for the CP-MC-EDFA over the respective 35-nm spectral windows from 1535 – 1570 nm and 1532 – 1567 nm.

The results shown in Fig. 15 and 16 indicate that, when it is possible to select the spectral region, CP-MC-EYDFAs offer a higher minimum gain compared to CP-MC-EDFAs since they use the pump more efficiently. However, the results also indicate that a deeper GFF is required.

VII. Conclusion

Through numerical simulations with parameters validated by experimental results with a single-core fiber, we investigated the benefits of using Er/Yb co-doping for a multi-core amplifier in order to achieve a higher minimum gain than with erbium ion doping only. All the simulations parameters are in agreement with typical values found in the literature. We first compared cladding pumped Er and Er/Yb doped amplifiers and found that Er/Yb co-doping could only be beneficial over the 1530-1560 nm spectral region in the specific case of a highly saturated amplifier, for example for low input pump power or high input signal power. Under these conditions Er/Yb co-doping can be advantageous because of its efficient absorption rate that leads to high population inversion levels even when available pump power is low. However, when the remaining output pump is reused [34], the benefits of Er/Yb co-doping might not be advantageous compared to Er-only doping since only a small fraction of pump light reaches the output of the fiber. Also, one of the drawbacks of using Er/Yb co-doping is the need for a deep GFF. However, when the 30-nm spectral window can be shifted to slight longer wavelengths, for example 1535 nm to 1565 nm, we also demonstrate that MC-CP-EYDFAs can reach much higher minimum gain than MC-CP-EDFAs. The results thus demonstrate that, although Er/Yb co-doping does not provide increased performance of MC-CP amplifiers in all scenarios, there can be important benefits of using co-doping in specific scenarios.

Acknowledgment

We would like to acknowledge the help of Mr N. Grégoire and Mr. Steeve Morency for the fiber fabrication and characterization.

National Science and Engineering Research Council of Canada (NSERC) Funding: RDCPJ 515551-17

REFERENCES

[1] Essiambre, R. J., Kramer, G., Winzer, P. J., Foschini, G. J., & Goebel, B. (2010). Capacity limits of optical fiber networks. *Journal of Lightwave Technology*, *28*(4), 662-701.

[2] Richardson, D. J., Fini, J. M., & Nelson, L. E. (2013). Space-division multiplexing in optical fibres. *Nature Photonics*, *7*(5), 354.

[3] K. S. Abedin, T. F. Taunay, M. Fishteyn, D. J. DiGiovanni, V. R. Supradeepa, J. M. Fini, M. F. Yan, B. Zhu, E. M. Monberg, and F. V. Dimarcello, "Cladding-pumped erbium-doped multicore fiber amplifier," Opt. Express **20**(18), 20191–20200 (2012).

[4] C. Jin, B. Huang, K. Shang, H. Chen, R. Ryf, R. J. Essiambre, N. K. Fontaine, G. Li, L. Wang, Y. Messaddeq, and S. Larochelle, "Efficient Annular Cladding Amplifier with Six, Three-Mode Cores," in European Conference on Optical Communication (ECOC, 2015), paper PDP2.1.

[5] Takeshima, K., Tsuritani, T., Tsuchida, Y., Maeda, K., Watanabe, K., Sasa, T., ... & Suzuki, M. (2015, March). 51.1-Tbit/s MCF transmission over 2,520 km using cladding pumped 7-core EDFAs. In *Optical Fiber Communication Conference* (pp. W3G-1). Optical Society of America.

[6] Jain, S., Mizuno, T., Jung, Y., Kang, Q., Hayes, J. R., Petrovich, M. N., ... & Isoda, A. (2016, September). 32-core inline multicore fiber amplifier for dense space division multiplexed transmission systems. In *ECOC 2016-Post Deadline Paper; 42nd European Conference on Optical Communication; Proceedings of* (pp. 1-3). VDE.

[7] Jain, S., Thipparapu, N. K., Barua, P., & Sahu, J. K. (2014). Cladding-pumped Er/Yb-doped multi-element fiber amplifier for wideband applications. *IEEE Photonics Technology Letters*, *27*(4), 356-358.

[8] Ono, H., Takenaga, K., Ichii, K., Matsuo, S., Takahashi, T., Masuda, H., & Yamada, M. (2013, September). 12-core double-clad Er/Yb-doped fiber amplifier employing free-space coupling pump/signal combiner module. In *Optical Communication (ECOC 2013), 39th European Conference and Exhibition on* (pp. 1-3). IET.

[9] Castro, C., Jain, S., De Man, E., Jung, Y., Hayes, J., Calabro, S., ... & Takenaga, K. (2017). 100-Gb/s transmission over a 2520-km integrated MCF system using cladding-pumped amplifiers. *IEEE Photonics Technology Letters*, *29*(14), 1187-1190.

[10] P. M. Krummrich and S. Akhtari, "Selection of energy optimized pump concepts for multi core and multi mode erbium doped fiber amplifiers," Opt Express, vol. 22, pp. 30267-80, Dec 1 2014.

[11] M. Nooruzzaman, S. Jain, Y. Jung, S. Alam, D. J. Richardson, Y. Miyamoto, et al., "Power Consumption in Multi-core Fibre Networks," in 2017 European Conference on Optical Communication (ECOC), 2017, pp. 1-3.

[12] Townsend, J. E., Barnes, W. L., & Crubb, S. G. (1991). Yb 3+ sensitised Er 3+ doped silica optical fibre with ultra high transfer efficiency and gain. *MRS Online Proceedings Library Archive*, *244*.

[13] Gapontsev, V. P., Matitsin, S. M., Isineev, A. A., & Kravchenko, V. B. (1982). Erbium glass lasers and their applications. *Optics & Laser Technology*, *14*(4), 189-196.

[14] Artem'ev, E. F., Murzin, A. G., Fedorov, Y. K., and Fromzel', V. A. (1981). Some characteristics of population inversion of the $^4I_{13/2}$ level of erbium ions in ytterbium–erbium glasses. Quantum Electronics, 11(9), 1266-1268.

[15] Hwang, B. C., Jiang, S., Luo, T., Watson, J., Sorbello, G., & Peyghambarian, N. (2000). Cooperative upconversion and energy transfer of new high Er 3+-and Yb 3+–Er 3+-doped phosphate glasses. JOSA B, 17(5), 833-839.

[16] Taccheo, S., Sorbello, G., Longhi, S., & Laporta, P. (1999). Measurement of the energy transfer and upconversion constants in Er–Yb-doped phosphate glass. Optical and quantum electronics, 31(3), 249-262.

[17] Grubb, S. G., Humer, W. F., Cannon, R. S., Windhorn, T. H., Vendetta, S. W., Sweeney, K. L., ... & Townsend, J. E. (1992). + 21 dBm erbium power amplifier pumped by a diode-pumped Nd: YAG laser. IEEE photonics technology letters, 4(6), 553-555.

[18] Yahel, E., & Hardy, A. (2003). Efficiency optimization of high-power, Er 3+–Yb 3+-codoped fiber amplifiers for wavelength-division-multiplexing applications. JOSA B, 20(6), 1189-1197.

[19] Vienne, G. G., Caplen, J. E., Dong, L., Minelly, J. D., Nilsson, J., & Payne, D. N. (1998). Fabrication and characterization of Yb3+: Er3+ phosphosilicate fibers for lasers. Journal of lightwave technology, 16(11), 1990.

[20] Valley, G. C. (2001). Modeling cladding-pumped Er/Yb fiber amplifiers. *Optical Fiber Technology*, *7*(1), 21-44.

[21] Vienne, G. G., Brocklesby, W. S., Brown, R. S., Chen, Z. J., Minelly, J. D., Roman, J. E., and Payne, D. N. (1996). Role of aluminum in ytterbium–erbium codoped phosphoaluminosilicate optical fibers. Optical Fiber Technology, 2(4), 387-393.

[22] Laporta, P., Taccheo, S., Longhi, S., Svelto, O., and Svelto, C. (1999). Erbium–ytterbium microlasers: optical properties and lasing characteristics. Optical Materials, 11(2-3), 269-288.

[23] Strohhöfer, C., and Polman, A. (2003). Absorption and emission spectroscopy in Er3+–Yb3+ doped aluminum oxide waveguides. Optical Materials, 21(4), 705-712.

[24] Philipps, J. F., Töpfer, T., Ebendorff-Heidepriem, H., Ehrt, D., and Sauerbrey, R. (2001). Spectroscopic and lasing properties of Er3+: Yb3+-doped fluoride phosphate glasses. Applied Physics B, 72(4), 399-405.

[25] Park, N., Wysocki, P., Pedrazzani, R., Grubb, S., DiGiovanni, D., & Walker, K. (1996). High-power Er-Yb-doped fiber amplifier with multichannel gain flatness within 0.2 dB over 14 nm. *IEEE Photonics Technology Letters*, *8*(9), 1148-1150.

[26] Jaouën, Y., Bouzinac, J. P., Delavaux, J. M., Chabran, C., & Le Flohic, M. (2000). Generation of four-wave mixing products inside WDM c-band 1 W Er^{3+}/Yb^{3+} amplifier. *Electronics Letters*, *36*(3), 233-235.

[27] Castro, C., Jain, S., De Man, E., Jung, Y., Hayes, J., Calabro, S., ... and Takenaga, K. (2018). 15×200 Gbit/s 16-QAM SDM Transmission Over an Integrated 7-Core Cladding-Pumped Repeatered Multicore Link in a Recirculating Loop. *Journal of Lightwave Technology*, *36*(2), 349-354.

[28] Nilsson, J., Scheer, P., & Jaskorzynska, B. (1994). Modeling and optimization of short Yb^{3+}-sensitized Er^{3+}-doped fiber amplifiers. *IEEE photonics technology letters*, *6*(3), 383-385.

[29] Peterka, P., Kanka, J., Karasek, M., Honzatko, P., & Abdelmalek, F. (1999, December). Characterization and modeling of Er/Yb-codoped fibers. In Photonics, Devices, and Systems (Vol. 4016, pp. 282-287). International Society for Optics and Photonics.

[30] Lester, C., Bjarklev, A., Rasmussen, T., & Dinesen, P. G. (1995). Modeling of Yb/sup 3+/-sensitized Er/sup 3+/-doped silica waveguide amplifiers. Journal of lightwave technology, 13(5), 740-743.

[31] K. S. Abedin, T. F. Taunay, M. Fishteyn, D. J. DiGiovanni, V. R. Supradeepa, J. M. Fini, M. F. Yan, B. Zhu, E. M. Monberg, and F. V. Dimarcello, "Cladding-pumped erbium-doped multicore fiber amplifier," Opt. Express **20**(18), 20191–20200 (2012).

[32] Ainslie, B. J. (1991). "A review of the fabrication and properties of erbium-doped fibers for optical amplifiers." Journal of Lightwave Technology, 9(2), 220-227. (1991)

[33] McCumber, D. E. (1964). Einstein relations connecting broadband emission and absorption spectra. *Physical Review*, *136*(4A), A954.

[34] Takeshita, H., Matsumoto, K., Yanagimachi, S., and de Gabory, E. L. T. (2019). Improvement of the Pump Recycling Ratio of Turbo Cladding Pumped MC-EDFA with Paired Spatial Pump Combiner and Splitter. In *Optical Fiber Communication Conference* (pp. Th1B-2).

National Science and Engineering Research Council of Canada (NSERC) Funding: RDCPJ 515551-17